



ISSN: 2321-2152

IJMECE

*International Journal of modern
electronics and communication engineering*

E-Mail

editor.ijmece@gmail.com

editor@ijmece.com

www.ijmece.com

Examination of Bones for Defects and Their Segmentation

¹G. Sudheer Kumar, ²S. Vasavi

¹Assistant Professor, Megha Institute of Engineering & Technology for Women, Ghatkesar.

²MCA Student, Megha Institute of Engineering & Technology for Women, Ghatkesar.

Abstract—

Bone diseases are common and may cause a variety of musculoskeletal ailments. An estimated 1.71 billion individuals around the globe deal with musculoskeletal disorders. Bone diseases are common and include musculoskeletal fractures, osteoarthritis of the knee, and femoral neck injuries. Conversely, a common prognostic failure in emergency situations is fractures that go unnoticed. Consequently, the care and treatment of patients becomes more convoluted and takes longer. There is a lot of excitement right now about the possibility that Deep Learning (DL) and Artificial Intelligence (AI) might aid doctors in detecting bone fractures. The use and promise of DL in the radiograph-based diagnosis of diseases and fractures have been shown in traumatology and orthopedics studies. The categorization of the bone has been examined in this research using several methods. The Inception-v3, VGG16, Densenet-121, and Resnet-50 algorithms are used for the identification and segmentation of wrist bones. As well as Resnet-50, Inception-v3, Densenet-121, and Densenet-169 for elbow bones. In the trials, two datasets—the Kaggle dataset and the MURA dataset—are employed. Densenet-169 outperformed the competing models on the MURA dataset, whereas Inception-v3 outperformed them on the Kaggle dataset, according to the experimental findings. Due to the vast variety of bone types, computer-assisted anomaly detection for bones is now crucial. Medical imaging using X-rays is the gold standard for diagnosing abnormalities in bones, especially after a fracture. Experts in the medical field rely on X-ray images to aid in making critical diagnoses. If the bone anomaly is misdiagnosed, it might lead to ineffective medical treatment, higher patient discontent, and expensive legal measures. Therefore, it is considered crucial to accurately identify these anomalies and treat them appropriately. A large number of recent research publications have focused on the topic of developing computer-aided techniques to detect bone fractures in different parts of the human body. The bulk of past research only considered one bone because of the vast variety of bone defects and the noticeable differences in bone

structure. This means an absurdly large number of systems would be required to cover every single bone in the human body.

Keywords— Medical imaging, Deep Learning, Resnet-50, VGG16, Densenet-121, Inception-v3, VGG16

INTRODUCTION

Many different areas of medicine have made use of medical imaging techniques. In terms of domain recognition, the X-rays domain is among the highest. The combination of radiation with computer image processing has led to the widespread usage of digital X-ray imaging systems in many medical contexts. Bone abnormality detection is a medical specialty that makes use of computer-aided diagnostics to assist in the identification of human bone abnormalities. Because the anomaly may manifest in any bone in the human body, diagnosing a bone abnormality is no easy task. Two bones of the upper extremities, the elbow and the wrist, are the focus of this article. This method is provided in two parts. The first step is determining whether the bone is aberrant or normal using X-ray scans. Stage 2 involves determining the kind of atypical bone fracture. The mentioned method employs a number of classifiers, including Inception-v3, VGG16, Densenet-121, and Resnet-50 for the bones of the wrist, and Resnet-50, Inception-v3, and Densenet-121 for the bones of the elbow. The MURA dataset, which was used in the first phase, and an another dataset from Kaggle, which includes different kinds of wrist and elbow fractures, which was utilized in the second phase. Here is how the rest of the paper is structured: Section 2 provides an overview of the relevant literature. The suggested approach is detailed in Section 3. The findings from the experiments are detailed in Section 4. In Section 5, the paper comes to a close.

RELATED WORK

There have been a number of recent studies that have shown the ability to detect bone anomalies, namely fractures, and even to determine the specific kind of fracture. This section offers a concise synopsis of the prior studies. In order to categorize anomalies in the top seven bones, X-ray bone abnormality detection using Mobile-Net Networks is suggested in [1]. Using the Mobile-Net Convolutional neural network (CNN), they demonstrated a two-step process for anomaly identification in bone X-rays. At first, X-ray pictures are classified as normal or abnormal using Mobile Net. Using data from a second Mobile-Net model, the second step goes even farther into categorizing the areas of interest from the first stage as different categories of anomalies. In order to enhance the X-ray pictures, the researchers use a number of pre-processing techniques. Among these methods are data improvement to increase the variety of the training dataset, picture resizing, and image normalization to scale pixel values. Image translation, resizing, and rotation are all part of data augmentation methods that provide more training examples. All seven bones averaged 73.42 percent accuracy using the MURA dataset, with the humerus achieving the highest accuracy at 86.5 percent. One study that utilized the MURA dataset to find abnormalities in X-ray bone scans was Solovyova et al. [2]. To identify anomalies in X-ray scans of the bones, they used a method based on deep learning. Employing the MURA dataset, which contains a vast array of bone radiographs? Following a fully connected layer classification of normal or abnormal X-ray images, the suggested technique uses a pre-trained ResNet-50 model to extract features. The authors also evaluated several data augmentation approaches with the aim of improving the model's functionality. The proposed method has an 80% success rate in identifying anomalies in X-ray pictures of the bones. A method for automatically detecting wrist fractures using poster anterior and lateral radiographs was suggested by Ebsim et al. [3]. They used a deep learning-based method to automatically detect wrist fractures from lateral and poster anterior radiographs. Of the 3718 wrist radiographs reviewed, 1077 were found to be negative and 2641 to be positive for wrist fractures. To automatically extract properties from input radiographs, the suggested technique employs a Convolutional neural network (CNN) model. By using a fully connected layer, the model subsequently classifies the radiographs as either showing a wrist fracture or not. Researchers also tested the suggested method in comparison to state-of-the-art models and evaluated the impact of data augmentation strategies

on the model's accuracy. The findings showed that the suggested method outperformed previous state-of-the-art models with an accuracy of 91%. Abhilash et al. [4] analyzed bone abnormalities such as infections and fractures using a Dense-Net Convolutional Neural Network for Abnormality Detection from X-Ray Bone Images. Using this dataset for training and evaluation, the researchers' Dense Net CNN was able to achieve an overall anomaly recognition accuracy of 94.7%. The researchers then tested their Dense-Net CNN against existing state-of-the-art methods for bone scan anomaly detection and found it to be superior. The study's findings, taken as a whole, point to the potential clinical diagnostic and therapeutic uses of Dense-net CNNs for anomaly detection in X-ray bone images.

PROPOSED METHOD

Fig. 1 shows that this research proposes a two-phase technique for the categorization of the wrist and elbow. Identifying and categorizing abnormalities in the bone (whether they be normal or pathological) is the primary function of the first stage. Determining the kind of elbow [8, 9, and 10] or wrist [5, 6, and 7] fracture is the goal of the second stage. Then, separate classifiers are used for each bone to determine the kind of fracture. The dataset and the steps of the proposed technique are thoroughly described in the sections that follow. Table A. In the MURA dataset, you may find 5,915 out-of-the-ordinary images and 9,067 typical ones [11, 12]. Here, we utilize the wrist dataset (3697 photos) and the elbow dataset (1912 images). A collection of pictures of the elbow and wrist is available on Kaggle. There are three distinct kinds of fractures in the Kaggle dataset: whole, partial, and dislocation. In the wrist data set, you'll find 117 test photographs in addition to 602 training images [13]. Furthermore, the elbow data contains 896 training photos and 150 testing images [14]. Because wrist and elbow anomalies are common and have major clinical implications, and because their detection may aid in precise diagnosis, treatment planning, and rehabilitation, these datasets were our primary focus. Although other bones of the upper extremities may also be investigated, there are particular benefits to studying the wrist and elbow from both a scientific and clinical perspective. Part B: Preprocessing is a crucial part of data science and deep learning initiatives. In order to facilitate analysis and modeling, it may help guarantee that the data is understandable, properly structured, and relevant. If machine learning is to enhance accuracy, decrease the danger of over-fitting, save modeling time and effort,

and promote interpretability, then data pretreatment is essential. Image augmentation is a method used by computer vision and machine teaching researchers to systematically increase the quantity and variety of a training dataset. The goal of image augmentation is to improve machine learning models' performance and generalizability by increasing the amount of training data available and introducing variations to the images. First, the photographs were all cropped to $224 \times 224 \times 3$ pixels. Then, several augmentation techniques were used, including random contrast, horizontal flipping, random gamma, and random brightness. Section C: Extracting and Recognizing Features the first step is to determine if two bones (the wrist and the elbow) are normal or not. Specifically, Resnet-50, Inception-v3, Densenet-121, and Densenet-169 are used for the elbow, while Inception-v3, VGG16, and Resnet-50 are utilized for the wrist. The categorization of images is accomplished using the Inception-v3 deep learning model. This architecture is an expansion of the original Inception, which was made to solve the problem of deep neural networks' computational efficiency and model size. The model's great performance and efficient use of computer resources with minimum increase in calculation load led us to choose it. An architecture based on Convolutional layers is used by Inception-v3.

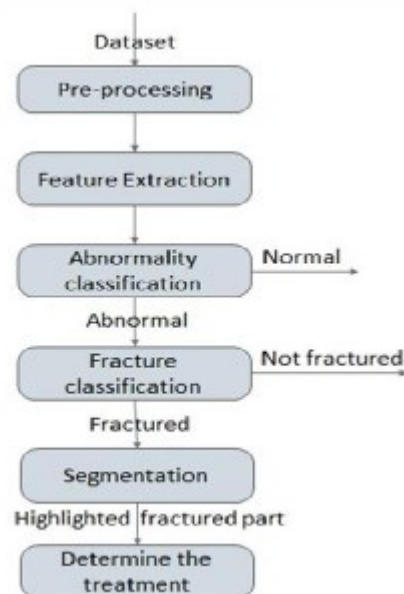


Fig.1. System architecture.

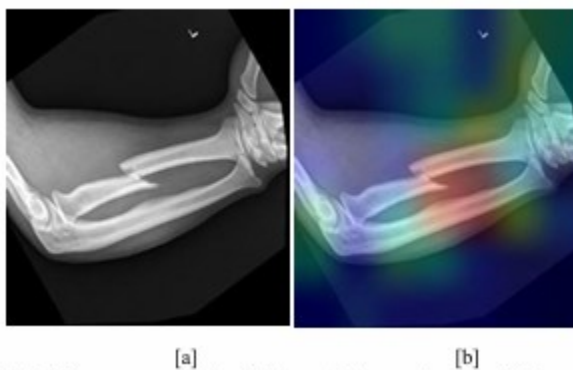
Layer blocks that execute multi-scale feature extraction, inception modules, and a range of filter sizes, and pooling layers. In order to provide a more

accurate representation of the input picture, these modules are built to extract characteristics at various spatial scales and combine them. To further enhance generalization performance and avoid over-fitting, regularization methods like dropout and batch normalization are used. The classification outputs are generated by the network's last layer, which is a soft-max activation function. Architecture of deep Convolutional neural networks (CNNs) is Densenet-169. The "Densely Connected Convolutional Network" configuration, which goes by the acronym "Dense-Net," is characterized by a feed-forward relationship between every layer of the network. Building on Dense-Net principles, DenseNet-169 design adds depth and intricacy. Each of the four dense blocks that make up the DenseNet-169 architecture has many levels of densely linked blocks. The first section consists of the max pooling layer and the Convolutional layer. In a dense block, each layer is connected to every layer before it using Convolutional neural networks. By facilitating information flow throughout the network, dense connections lower the number of parameters required to train the model, which in turn improves accuracy and decreases the likelihood of over-fitting. The last layer of the network is a global average pooling layer that combines all of the feature vectors from the preceding layers into one. The final classification output is obtained by feeding this vector into a fully connected layer that uses a soft-max activation function. When bones are found to be aberrant, the second step is to determine whether they have a complete fracture, an incomplete fracture, or a dislocation fracture. In this case, we use the Resnet-50 model, CNN architecture with deep Convolutional layers. The networks make use of the starting weights from the Image-Net dataset. "Res-Net" means "Residual Network," and 50 indicates that the network has 50 levels. There are a total of fifty layers in the ResNet-50 design, including Convolutional layers, batch normalization layers, activation functions (often ReLU), and fully linked layers. Stronger representation capacity and improved classification accuracy are associated with deeper hierarchies in the ResNet-50 architecture. Section D: Dividing as previously stated, the output picture is segmented following the two steps of classification, as shown in Figure 2. We utilized Gradient weighted Class Activation Mapping (Grad-CAM) [15], a computer vision approach that may be used to show the parts of a picture or feature map that are most important for a certain neural network classification decision. Grad CAM relies on the gradient information of a neural network's output with regard to a particular class to create a class activation map. This map then draws attention to the portions of the

input picture that are crucial for making a classification decision.

EXPIREMENTAL RESULTS

Horizontal flipping, random contrast, shift scale rotation, and normalization are the preprocessing steps used on the MURA dataset. Finding out whether the bone is aberrant or normal is the goal of the first round of tests. While the first batch determines the aberrant bone's abnormality kind, the second batch determines the fracture type. Phase 1 (abnormality identification) end result Resnet-50, VGG16, Densenet-121, and Inception-v3 are some of the approaches utilized for wrist bone segmentation. Densenet-121, Resnet-50, Inception-v3, and Densenet-169 are used for the elbow bone. In Table I, we can see how well the various recognition techniques performed on the MURA dataset. After comparing several models, the findings reveal that Inception-v3 obtained the greatest accuracy at 84% for the wrist bone and that the Densenet-169 model earned the best accuracy at 86% for the elbow bone. While testing on the MURA dataset, these two models proved to be the most effective. When the wrist bone is segmented using Inception-v3, the confusion matrix is shown in Figure 3. Table II displays the results of the Inception-v3 wrist bone segmentation task, including the recall, precision, and F1-score. Figure 4 displays the Densenet-169 elbow bone segmentation confusion matrix. Noted in Table III are Densenet-169's recall, accuracy, and F1-score as they pertain to elbow bone segmentation. (B) Findings from the second phase (identification of fracture types) The Kaggle dataset uses a variety of approaches for wrist bone segmentation, including VGG16, Densenet-121, Le-net, and



[A] [B] Fig. 2. Image segmentation: (a) image before grad-cam and (b) image after applying grad-cam to highlight fracture.

TABLE I. RESULTS OF ABNORMALITY DETECTION USING MURA DATASET.

Bones	Models	Accuracy
Wrist	Resnet-50	68%
	VGG16	72%
	Densenet-121	76%
	Inception-v3	84%
Elbow	Resnet-50	65%
	Densenet-121	73%
	Inception-v3	83%
	Densenet-169	86%

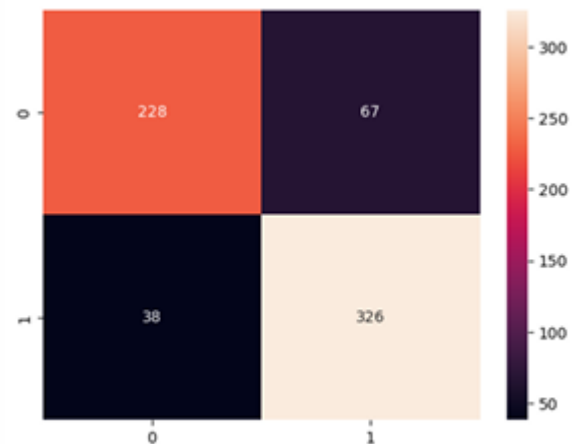


Fig. 3 The confusion matrix of using Inception-v3 to segment the wrist bone.

TABLE II. THE RECALL, PRECISION AND F1-SCORE FOR USING INCEPTION-V3 TO SEGMENT THE WRIST BONE.

	recall	precision	f1-score	support
class 0	0.77	0.86	0.81	295
class 1	0.90	0.83	0.86	364
accuracy			0.84	659

In the Kaggle dataset, Resnet-50 is used for the elbow bone, in addition to VGG16 and Densenet-121. Table IV provides a summary of the findings for detecting fracture types in each bone individually. Resnet-50 outperformed the competing models on the Kaggle dataset when it came to segmenting bones and wrists.

Figure 5 displays the confusion matrix for the Kaggle dataset when the wrist bone is segmented using Resnet-50. The results of the Resnet-50 wrist bone segmentation task, including recall, precision, and F1-score, are shown in Table V. Figure 6 displays the confusion matrix for the Kaggle dataset's elbow bone segmentation using Resnet-50. The recall, accuracy, and F1-score for the elbow bone segmentation using Resnet-50 are shown in Table VI.

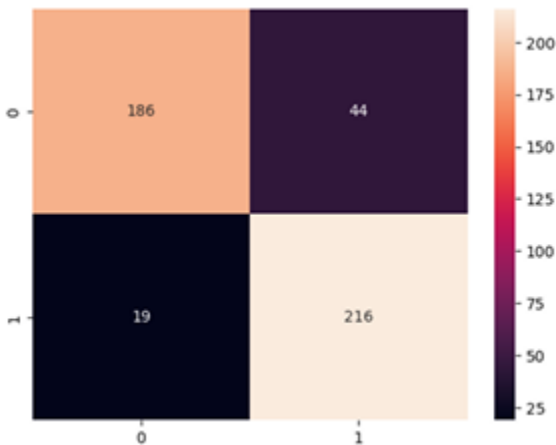


Fig. 4. The confusion matrix of using Densenet-169 to segment the elbow bone.

TABLE III. THE RECALL, PRECISION AND F1-SCORE FOR DENSENET 169 TO SEGMENT THE ELBOW BONE.

	recall	precision	f1-score	supp
class 0	0.81	0.91	0.86	230
class 1	0.92	0.83	0.87	235
accuracy			0.86	465

TABLE IV RESULTS OF FRACTURE TYPE DETECTION USING KAGGLE DATABASE.

Bones	Models	Accuracy
Wrist	VGG16	54%
	Densenet-121	64%
	Le-net	56%
	Resnet-50	92%
Elbow	VGG16	55%
	Densenet-121	62%
	Resnet-50	91%

First, using the MURA dataset, we assess the performance of several Convolutional neural network (CNN) models on two datasets: the wrist dataset and the elbow dataset, respectively. These models include the Inception-v3 and Densenet-169 networks. The kind of fracture is identified in the second step. When applying the MURA dataset to the elbow and wrist bones, correspondingly, an accuracy of 86% and 84% was attained. In addition, the wrist bone attained 92% accuracy and the elbow bone 91% accuracy while utilizing the Kaggle dataset. The study tested two of the seven bones that make up the upper limb—the wrist and the elbow—rather than the one bone that had previously been the subject of inquiry.

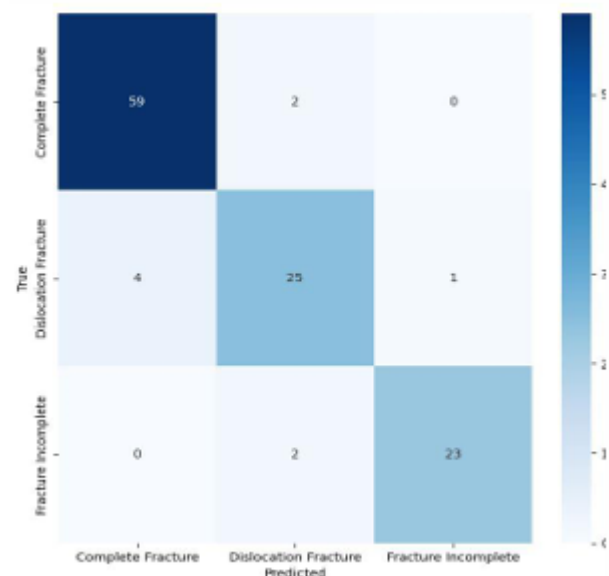


Fig. 5. The confusion matrix of using Resnet-50 to segment the wrist bone in the Kaggle dataset.

TABLE V. THE RECALL, PRECISION AND F1-SCORE FOR USING RESNET-50 TO SEGMENT THE WRIST BONE IN THE KAGGLE DATASET.

CONCLUSION

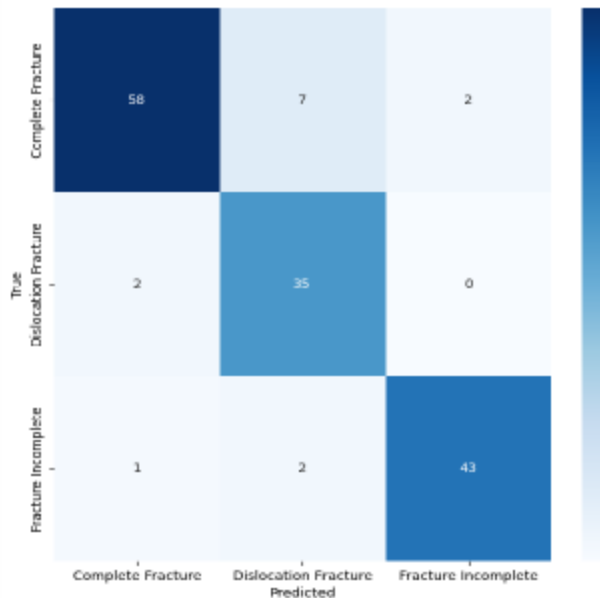


Fig. 6 the confusion matrix of using Resnet-50 to segment the elbow bone in the Kaggle dataset

TABLE VI. THE RECALL, PRECISION AND F1-SCORE FOR USING RESNET-50 TO SEGMENT THE ELBOW BONE IN THE KAGGLE DATASET.

	recall	precision	f1-score	support
Complete Fracture	0.87	0.95	0.91	67
Dislocation Fracture	0.95	0.80	0.86	37
Fracture Incomplete	0.93	0.96	0.95	46
accuracy			0.91	115

REFERENCES

- [1]. 115 Hadeer El-Saadawy, Manal Tantawi, Howida A. Shedeed, Mohamed Tolba, "A two-stage method for bone X-rays abnormality detection using mobileNet network." International Conference on Artificial Intelligence and Computer Vision (AICV2020). Springer International Publishing, 2020.
- [2]. Anna Solovoya, Igor Solovyov, TraumAI, "X-Ray Bone Abnormalities Detection Using ArXiv: 2008.03356 [Cs, Eess], 7 Aug. 2020. MURA Dataset."
- [3]. Raja Ebsim, Jawad Naqvi, and Timothy F. Cootes, "Automatic detection of wrist fractures from posteroanterior and lateral radiographs: a deep learning-based approach," Computational Methods and Clinical Applications in Musculoskeletal Imaging: 6th International Workshop, MSKI 2018, Held in Conjunction with MICCAI 2018, Granada, Spain, September 16, 2018, Springer International Publishing, 2019.
- [4]. Abhilash, Shukla, and Patel Atul, "Abnormality Detection from X Ray Bone Images Using DenseNet Convolutional Neural Network," International Journal of Current Research and Review, vol. 13, no. 10, 2021, pp. 101–106, Accessed 3 Apr. 2022.
- [5]. Pranav Rajpurkar, Jeremy Irvin, Aarti Bagul, Daisy Ding, Tony Duan, Hershel Mehta, Brandon Yang, Kaylie Zhu, Dillon Laird, Robyn L. Ball, Curtis Langlotz, Katie Shpanskaya, Matthew P. Lungren, Andrew Y. Ng, "Mura: Large dataset for abnormality detection in musculoskeletal radiographs," arXiv:1712.06957, 2017.
- [6]. Abu Mohammed Nevalainen, Marko Raisuddin, Elias Nikki, Elina Vaattovaara, Mika Järvenpää, Kaisa Makkonen, Pekka Pinola, Tuula Palsio, Arttu Niemensivu, Osmo Tervonen, and Aleksei Tiulpin "Critical evaluation of deep neural networks for wrist fracture detection," Scientific reports 11, Article number: 6006, 2021.
- [7]. Weijie Huang, Fuqiang Sun, Menghua Zhang, Yongfeng Zhang, Changhui Ma, "Data Enhancement for Deep Learning-Based Wrist Fracture Detection," Lecture Notes in Electrical Engineering Advances in Applied Nonlinear Dynamics, Vibration and Control, pp. 1182-1193, 2021.
- [8]. Doornberg, Job N., Thierry G. Guitton, and David Ring, "Diagnosis of elbow fracture patterns on radiographs: interobserver reliability and diagnostic accuracy," Clinical Orthopaedics and Related Research, vol 471, No. 4, pp. 1373-1378, 2013.
- [9]. Sun Hwa Lee MD, Seong Jong Yun MD, "Diagnostic Performance of Ultrasonography for Detection of Pediatric Elbow Fracture: A Meta-analysis," Annual of Emergency Medicin, vol 74, Issue 4, 2019
- [10]. Mehmet Birkan Korgan, Yusuf Ali Altuncu, İlhan Uz, Funda Karbek Akarca, "Effectiveness of ultrasonography

performed at the emergency department for pediatric elbow trauma cases, Injury, vol 54, Issue 11, 111005, 2023

- [11]. Jesse C. Rayan, Nakul Reddy, J. Herman Kan, Wei Zhang, Ananth Annapragada, "Binomial classification of pediatric elbow fractures using a deep learning multiview approach emulating radiologist decision making." Radiology Artificial Intelligence, vol 1, no. 1, e180015, 2019.
- [12]. MURA dataset:
<https://stanfordmlgroup.github.io/competitions/mura>
- [13]. Wrist data:
<https://www.kaggle.com/datasets/samsamalgzar/wristttt>.
- [14]. Elbow data:
<https://www.kaggle.com/datasets/maramhateem/elbow-final>
- [15]. Nicola Altini, Antonio Brunetti, Emilia Puro, Maria Giovanna Taccogna, oncetta Saponaro, Francesco Alfredo Zito, Simona De Summa, and Vitoantonio Bevilacqua, "NDG-CAM: nuclei detection in histopathology images with semantic segmentation networks and grad-CAM," Bioengineering, vol. 9, no. 9, 475, 2022.